6984–6994 *Nucleic Acids Research, 2007, Vol. 35, No. 20* *Published online 16 October 2007*
doi:10.1093/nar/gkm703

Crystal structure of the human FOXO3a-DBD/DNA complex suggests the effects of post-translational modification

Kuang-Lei Tsai[1,2], Yuh-Ju Sun[2], Cheng-Yang Huang[1], Jer-Yen Yang[3], Mien-Chie Hung[3,4] and Chwan-Deng Hsiao[1,*]

[1]Institute of Molecular Biology, Academia Sinica, Taipei, 115, [2]Institute of Bioinformatics and Structural Biology, National Tsing Hua University, Hsinchu 30043, Taiwan, [3]Department of Molecular and Cellular Oncology, The University of Texas M. D. Anderson Cancer Center, Houston, TX 77030, USA, and [4]Center for Molecular Medicine, China Medical University Hospital, Taichung, 404, Taiwan.

Received June 4, 2007; Revised August 17, 2007; Accepted August 23, 2007

ABSTRACT

FOXO3a is a transcription factor of the FOXO family. The FOXO proteins participate in multiple signaling pathways, and their transcriptional activity is regulated by several post-translational mechanisms, including phosphorylation, acetylation and ubiquitination. Because these post-translational modification sites are located within the C-terminal basic region of the FOXO DNA-binding domain (FOXO-DBD), it is possible that these post-translational modifications could alter the DNA-binding characteristics. To understand how FOXO mediate transcriptional activity, we report here the 2.7 Å crystal structure of the DNA-binding domain of FOXO3a (FOXO3a-DBD) bound to a 13-bp DNA duplex containing a FOXO consensus binding sequence (GTAAACA). Based on a unique structural feature in the C-terminal region and results from biochemical and mutational studies, our studies may explain how FOXO-DBD C-terminal phosphorylation by protein kinase B (PKB) or acetylation by cAMP-response element binding protein (CBP) can attenuate the DNA-binding activity and thereby reduce transcriptional activity of FOXO proteins. In addition, we demonstrate that the methyl groups of specific thymine bases within the consensus sequence are important for FOXO3a-DBD recognition of the consensus binding site.

INTRODUCTION

The forkhead box proteins (FOX proteins) comprise a large family of functionally diverse transcription factors involved in cellular proliferation, transformation, differentiation and longevity (1–3). These proteins, found in various species ranging from yeast to human, have multiple domains that are specific for DNA binding, transactivation or transrepression (4). One sub-family of FOX proteins, the 'O' class forkhead proteins (FOXO), are transcription factors that play important roles in several biological processes, including metabolism, cellular proliferation, cell survival and response to oxidative stress (5–10). To date, the FOXO family in mammals contains four members: FOXO1 (FKHR), FOXO3a (FKHRL1), FOXO4 (AFX) and FOXO6. These proteins share a high degree of evolutionary conservation, especially in the forkhead DNA-binding domain (Figure 1A and B) (11–14). Among these FOXO proteins, FOXO3a is involved in cell transformation, tumor progression and angiogenesis (15–17).

FOXO proteins participate in multiple signaling pathways, and their transcriptional activity is regulated by several post-translational mechanisms, including phosphorylation, acetylation and ubiquitination (16,18–21). All FOXO proteins are regulated by insulin or growth factor signaling through the phosphatidylinositol 3-kinase–protein kinase B (PI3K–PKB) pathway (20,22,23). PKB-induced phosphorylation of FOXO proteins generates two binding sites for the binding of 14-3-3 proteins, which results in the translocation of FOXO/14-3-3 complex from the nucleus to the cytoplasm (20,24). In addition, the binding of 14-3-3 proteins to FOXO is required for FOXO protein dissociation from DNA and prevents re-translocation of FOXO into the nucleus by masking the function of the nuclear localization sequence (NLS) (20,25–29). Recent studies have shown that acetylation of FOXO proteins by cAMP-response element binding (CREB)-binding protein (CBP) and deacetylation by Sir2 are also important regulators of FOXO-mediated transcriptional activity (21,30–33).

*To whom correspondence should be addressed. Tel: +886 2 2788 2743; Fax: +886 2 2782 6085; Email: hsiao@gate.sinica.edu.tw

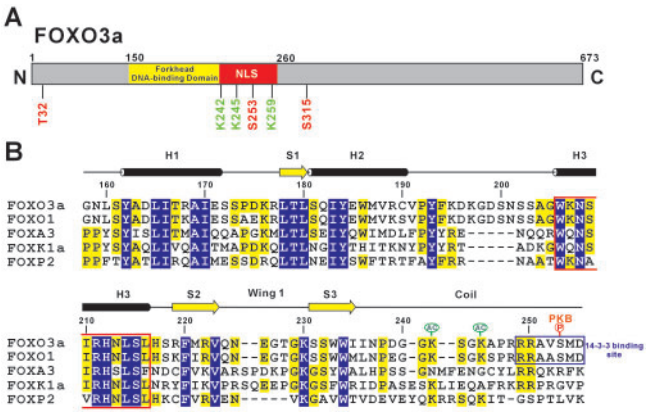

Figure 1. Schematic representation of FOXO3a and sequence alignment of its forkhead domain with other FOX proteins. (**A**) Schematic domain structure of FOXO3a. Forkhead domain and NLS are colored yellow and red, respectively. (**B**) Sequence alignment of the forkhead DNA-binding domains from FOXO3a, FOXO1, FOXA3, FOXK1a and FOXP2 are shown with reference to the residue numbers and secondary structural elements of FOXO3a (black cylinders, α-helices; yellow arrows, β-strands). The amino acids of helix 3 that are highly conserved in the winged helix/forkhead family are boxed in red. Residues that are identical or similar among family members are shaded in blue and yellow, respectively.

In FOXO1, CBP-induced acetylation at two basic residues, Lys242 and Lys245 (corresponding to Lys242 and Lys245 in FOXO3a), located in the C-terminal region of the DNA-binding domain, has been shown to reduce its DNA-binding affinity and transcriptional activity (21,34).

Each member of the FOX family contains a conserved DNA-binding domain (forkhead domain) with a winged-helix fold that recognizes DNA. This so-called 'winged helix/forkhead domain' contains ~100 conserved amino acid residues and is characterized by three α-helices packed against each other, three small β-strands, one wing known as 'wing 1' and the C-terminal α-helix or 'wing 2' (35–41). To date, the crystal structures of the forkhead DNA-binding domain bound to DNA have been determined for FOXA3 (also named HNF-3γ), FOXK1a and FOXP2 (Figure 1B) (35,36,41). Although the DNA-binding domains of FOX proteins share a high degree of sequence homology in the recognition helix (helix 3), their DNA recognition specificity shows notable variations (38,42,43). The amino acid compositions in the H2–H3 turn, wing 1 and C-terminal region of the DNA-binding domain exhibit apparent sequence deviations. Thus, it has been hypothesized that the variability in DNA recognition specificity is modulated by these non-conserved DNA-binding domain regions (42,43).

Because the PKB phosphorylation site (Ser253), CDK2 phosphorylation site (Ser246 in FOXO1) and CBP acetylation sites (Lys242 and Lys245) are located within the C-terminal basic region of the FOXO DNA-binding domain, it is possible that these post-translational modifications could alter the DNA-binding characteristics by introducing a negative charge or disrupting protein–DNA contacts in this region that result in destabilization of the protein–DNA complex. Hence, the elucidation of the FOXO–DNA complex structure is necessary to understand the molecular basis for FOXO protein recognition of DNA. Here, we report the 2.7 Å resolution crystal structure of the DNA-binding domain of FOXO3a (FOXO3a-DBD) bound to a 13-bp DNA duplex containing a FOXO consensus binding sequence. Based on a structural feature in the C-terminal region of FOXO3a-DBD, as well as results from biochemical and mutation studies, we discuss the potential phosphorylation and acetylation sites for the C-terminal region of FOXO3a-DBD.

MATERIALS AND METHODS

Expression and purification of FOXO3a-DBD

DNA encoding residues 158–253 of human FOXO3a-DBD was generated by PCR amplification using full-length FOXO3a cDNA and ligated into pET-21b using the NdeI and XhoI sites. The R211A, K230A, K242A, K245A, KK (double mutant, K242A and K245A), A246D and RRR (triple mutation, R248A, R249A and R250A) mutants were generated according to the QuickChange mutagenesis protocol (Stratagene, La Jolla, CA, USA) using the pET-21b-FOXO3a-DBD wild-type plasmid as the template. The C-terminally truncated FOXO3a-DBD (residues 158–240) was generated by introducing a stop codon before Gly241. All mutant constructs were verified by DNA sequencing. The recombinant protein contained only one additional residue (Met) at the N-terminus. Recombinant FOXO3a-DBD was expressed in an *Escherichia coli* system and induced by addition of IPTG at a final concentration of 1 mM for 3 h at 37°C. The lysate was clarified by centrifugation, and the resulting supernatant was loaded onto a heparin-Sepharose column (Amersham Biosciences) equilibrated in buffer containing 25 mM HEPES (pH 6.5), 100 mM NaCl and 1 mM DTT. FOXO3a-DBD was eluted using a linear gradient of NaCl (100–1000 mM). Eluted protein was then purified by gel-filtration chromatography on a Superdex75 column (Amersham Biosciences) in 25 mM HEPES (pH 7.2), 100 mM NaCl and 1 mM DTT. Peak fractions were pooled and concentrated to ~20 mg/ml for storage at −80°C.

Crystallization of protein–DNA complex

Complementary oligonucleotides (5′-CTATGTAAACAA C-3′ and 5′-GTTGTTTACATAG-3′) with 13 bases per single strand were purchased from MdBio, Inc. (Frederick, MD), and annealed as described (36). FOXO3a-DBD was mixed with the oligonucleotides at a 1:1 molar ratio at a final protein concentration of 5 mg/ml in buffer containing 25 mM HEPES (pH 7.2), 2 mM DTT and 150 mM NaCl. Crystals were grown at 20°C using the hanging drop vapor diffusion method. The protein–DNA complex was mixed with an equal volume of reservoir solution containing 100 mM Bis–Tris (pH 7.4), 50 mM $MgCl_2$ and 30% PEGMME 550. The crystals grew up to $0.3 \times 0.3 \times 0.1$ mm^3 in size in 2–3 days.

Data collection and structure determination

A crystal was soaked in reservoir solution containing 25% glycerol for 25 min before flash cooling in liquid nitrogen.

A complete data set was collected on an ADSC Quantum 4R CCD detector using the synchrotron radiation X-ray source at Beamline 13B1 of the National Synchrotron Radiation Research Center (NSRRC) in Taiwan. All data were processed with the HKL2000 package (44). The crystal belonged to the $P6_1$ space group, with unit cell dimensions $a = b = 41.9$ Å and $c = 354.8$ Å, and diffracted to 2.7 Å resolution.

The structure of the FOXO3a-DBD/DNA complex was determined using the molecular replacement method by the MolRep program (45). Initial phases were obtained at 4 Å resolution using the coordinates of FOXK1a (PDB code: 2C6Y) as a search model, yielding a solution with a correction coefficient of 45% and an R_{factor} of 40%. XtalView (46) was used to examine electron density maps and for model building. The refinement and final analysis were performed with CNS (47). Water molecules were added with a water-pick routine in the CNS program. The current model has an R-factor of 24.1% for all reflections between 25 and 2.7 Å resolution and an R_{free} of 26.6%, using 5% randomly distributed reflections. In the current model, 84% of all residues are in the most favored region of the Ramachandran plot, and no residues are in the disallowed region. The helical parameters of DNA were analyzed using the CURVE (48) program. The figures were generated using the PyMol (49) program. The data collection and refinement statistics are presented in Table 1.

Table 1. Crystallographic data

Data collection and refinement statistics	
Crystal	FOXO3a-DBD/DNA
Wavelength (Å)	1.0000
Resolution (Å)	25–2.7
Space group	$P6_1$
Cell dimension (Å)	$a = 41.9$ $c = 354.8$
Completeness (%)	97.1 (97.3)[a]
$\langle I\sigma I\rangle$	40.2 (2.7)
R_{sym}[b]	5.1 (42.4)
Redundancy	4.2
Refinement	
Resolution (Å)	25–2.7
Number of reflections	9125
R_{work}/R_{free}	24.2/26.6
No of atoms	
Protein	1478
DNA	1054
Water	209
B-factors	
Protein	24.4
DNA	17.0
Water	18.7
RMSD	
Bond lengths (Å)	0.012
Bond angles (°)	2.6

[a]Highest resolution shell is shown in parenthesis (2.87–2.70 Å for the native data set).
[b]R_{sym} $(I) = \Sigma_h\Sigma_i|I_i - I|/\Sigma_h\Sigma_i I$, where I is the mean intensity of the i observations of reflection h.

Electrophoretic mobility shift assay

A 26-bp DNA fragment containing the FOXO consensus sequence (5′-CGCATCCTATGTAAACAACTCGA GTC-3′), and each of the mutant oligonucleotides, were ^{32}P-labeled at the 5′ terminus with T4 polynucleotide kinase and [γ-^{32}P] ATP (New England Biolabs). The labeled probe was incubated with 10, 20 or 50 ng of FOXO3a-DBD in a total volume of 20 µl in 25 mM HEPES, pH 7.0, 50 mM NaCl, 1 mM DTT, 1 mM $MgCl_2$, 1 mg/ml BSA and 20 ng of poly(dI-dC). After a 40-min incubation on ice, the binding reactions were directly loaded onto a native 10% polyacrylamide gel and electrophoresed in 0.5× TBE buffer (1× TBE contains 89 mM Tris, pH 8.3, 89 mM boric acid and 2 mM EDTA). The gels were dried and quantified by phosphorimaging.

Fluorescence anisotropy assay

The dissociation constants of FOXO3a-DBD proteins for FOXO consensus DNA were determined using a fluorescence anisotropy assay. Fluorescence anisotropy measurements were performed in a Fluorolog-3 spectrometer (Jobin Yvon Inc.) with polarizers placed in L-format. The measurements were taken at an excitation wavelength of 490 nm and emission wavelength of 520 nm. Dilutions of FOXO3a-DBD proteins were incubated with a 26-bp DNA duplex with a 5′-fluorescein label on one strand of the DNA duplex at room temperature for 30 min. The DNA concentration was 1 nM. All binding reactions were carried out in 1 ml of binding buffer containing 20 mM Tris–HCl, pH 7.6, 50 mM NaCl and 1 mM DTT. The anisotropy of each sample was measured at 25°C. Three to six measurements were collected and averaged for each point of the binding isotherm. The dissociation constant (K_d) values of wild-type and mutant FOXO3a-DBD proteins for the 26-bp DNA were derived from anisotropy data converted into fraction of DNA bound as a function of FOXO3a-DBD concentration.

RESULTS

Overview of the FOXO3a-DBD/DNA complex

We determined the crystal structure of FOXO3a-DBD (residues Gly158 to Ser253) bound to a 13-bp duplex DNA containing the 7-bp FOXO consensus binding sequence (GTAAACA) at 2.7 Å resolution (Figure 2). In the asymmetric unit of the crystal, two FOXO3a-DBD molecules bound to two DNA duplexes with a pseudo 2-fold symmetry (Figure 2A). The geometry of the DNA duplex was canonical B-form DNA with a few kinks. In the crystal, the DNA duplexes formed a pseudo-continuous DNA helix stabilized by base-stacking interactions with symmetry-related DNA. There were direct protein–protein interactions between the two FOXO3a-DBD molecules, ostensibly forming a homodimer; however, to date no biological function has been ascribed for such a dimer of FOXO3a-DBD.

The two FOXO3a-DBD molecules bound to DNA in a similar manner. Briefly, the DNA-binding domain of FOXO3a was arranged in a compact winged-helix motif consisting of three α-helices, three β-strands, one wing (wing 1) and a C-terminal coil (Figure 2C). The recognition helix (H3) docked into the major groove

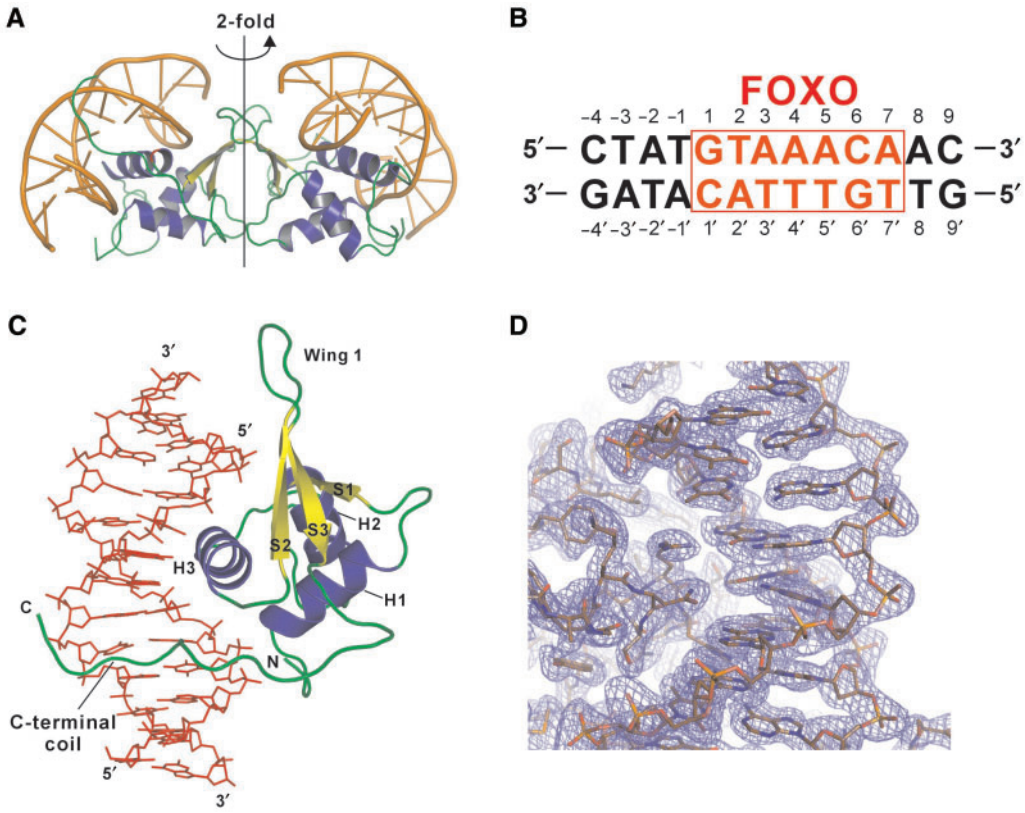

Figure 2. Overall structure of the FOXO3a-DBD/DNA complex. (**A**) The dimeric structure of FOXO3a-DBD/DNA complex with a pseudo 2-fold symmetry within an asymmetric unit. Two FOXO3a-DBD molecules are shown as ribbon drawings with the DNA in orange. (**B**) Sequence of the 14-bp DNA duplex used in crystallization. Nucleotides colored red are the FOXO consensus sequence. (**C**) The complete structure of FOXO3a-DBD/DNA complex. The secondary structure elements and the N and C termini of FOXO3a-DBD are labeled. The 14 bp DNA is colored red. H and S are abbreviations for helix and strands, respectively. (**D**) The $2F_o$–F_c electron density map contoured at 1.0σ at the interface between the recognition helix and major groove of DNA in the FOXO3a-DBD/DNA complex.

roughly perpendicular to the DNA axis and made numerous interactions with the FOXO consensus sequence. The protein–phosphate interactions were localized in two phosphate backbones forming the major groove of the core sequence. In the region between H2 and H3, the residues preceding the recognition helix formed a solvent-exposed loop structure. The typical wing 1 interacted with the phosphate group of the 3′ flanking region of the consensus sequence without making base-specific contacts. In the C-terminal region of FOXO3a-DBD, the residues following S3 formed a coil structure that aligned to the major groove and interacted with the DNA (Figure 2C). To analyze structural deviations, two FOXO3a-DBD molecules related by pseudo 2-fold symmetry in the asymmetric unit were superimposed. The 0.64 Å root mean square deviation (RMSD) for Cα atoms of secondary structural elements showed no obvious structural disparity. Figure 2D shows the electron density map of the interface between the recognition helix and major groove of DNA.

Major groove recognition within the consensus binding site

In most forkhead proteins, the recognition helices H3 within the DNA-binding domain share a highly conserved amino acid sequence (Figure 1B). As expected, the recognition helix H3 in the FOXO3a-DBD structure docked perpendicular to the major groove and formed extensive contacts with the FOXO consensus binding sequence. The recognition helix H3 centered over the FOXO consensus sequence, with several residues within helix 3 forming direct hydrogen bonds as well as van der Waals contacts with bases of the major groove. Details of the interactions between recognition helix H3 and DNA are shown in Figures 3A and 4. The conserved residues Asn208, Ser215, Arg211 and His212 within H3 were important for DNA recognition. Asn208 bound to the A4 base via two hydrogen bonds. Arg211 recognized T5′ and T7′ through van der Waals contacts and contributed to the specificity for G6′ with a direct hydrogen bond. The side chain of His212 protruded into the major groove and recognized bases T2 and T3′ through a van der Waals contact and a direct hydrogen bond, respectively. Ser215 recognized T4′ through a van der Waals contact. Among these interactions, we note that the methyl groups of thymine bases from the FOXO consensus binding sequence were crucial for FOXO3a-DBD promoter recognition. In addition to base recognition, Ser215 also interacted with the phosphate group of T8′ to further stabilize the complex.

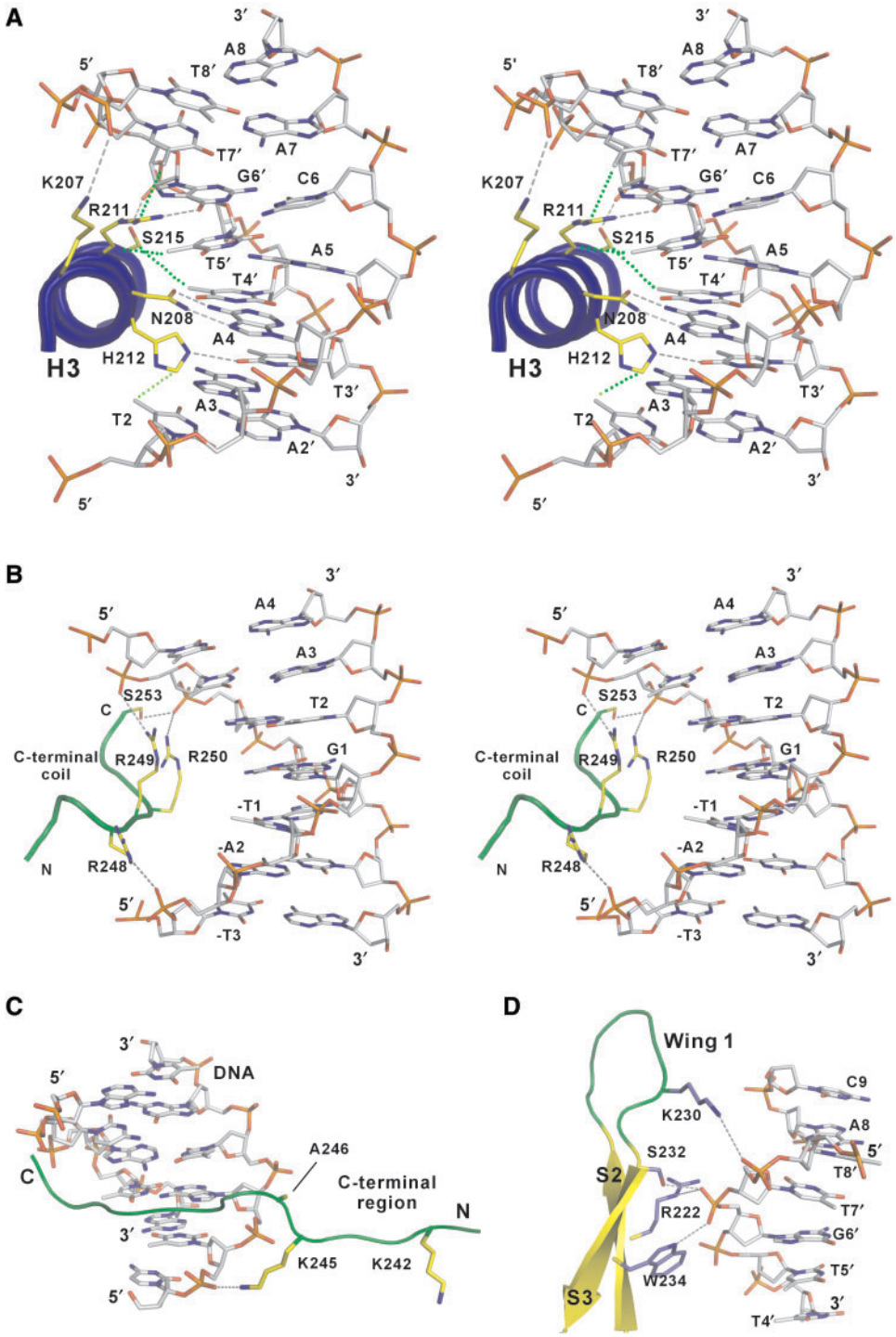

Figure 3. Detailed contacts of the FOXO3a-DBD/DNA interface. (**A**) Stereo view of the recognition of the GTAAACA consensus DNA-binding sequence by recognition helix H3 of FOXO3a-DBD. Hydrogen bonding and van der Waals contacts participating in base recognition are represented by dashed gray lines and dotted green lines, respectively. (**B**) Stereo view of major groove interactions of the C-terminal region of FOXO3a-DBD. Hydrogen bonds are represented by dashed gray lines. The C-terminal coil of FOXO3a-DBD is colored in green. (**C**) Interactions between DNA and the C-terminal positively charged Lys245 residue. (**D**) Interactions between wing 1 of FOXO3a-DBD and the minor groove of DNA are shown.

The FOXO3a-DBD C terminus forms a coil to interact with the DNA major groove

In the FOXO3a-DBD/DNA complex, the C-terminal region adopted a coil structure and interacted with the major groove of DNA (Figures 2C and 3B). Interestingly, the C-terminal region (242-KSGKAPRR RAVS-253) not only functions as a NLS, but also overlaps with the PKB phosphorylation site, 14-3-3 binding motif and CBP acetylation sites (Figure 1A and B) (20,21,34). The three basic residues Arg248-Arg249-Arg250, part of

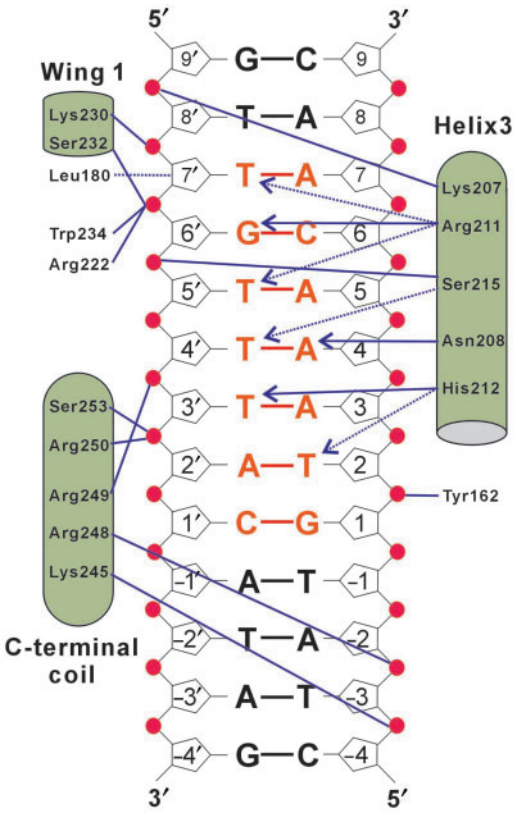

Figure 4. Schematic diagram of interactions between FOXO3a-DBD and DNA. The phosphate groups of DNA are represented as red circles. Base pairs of the FOXO consensus DNA-binding sequence, GTAAACA, are in red. The residues of helix 3, wing 1 and the C-terminal coil that make contacts with DNA are boxed in green. Hydrogen bonding and van der Waals contacts participating in base recognition are represented by thin arrowed lines and dotted lines, respectively. Hydrogen bonds and van der Waals contacts to DNA backbones are represented by thin lines and dotted lines without arrows, respectively.

the PKB recognition motif, are highly conserved in other members of the FOXO family. In our structure, this region played an important role in DNA major groove binding, with each of these three residues forming an ion pair with a phosphate group in the major groove of the DNA backbone without base-specific contacts (Figure 3B). Ser253, a PKB phosphorylation site, immediately following the Arg248–250 motif also made direct contact with a DNA phosphate group (Figure 3B), implying that Ser253 (when non-phosphorylated) participates in DNA binding. PKB-mediated phosphorylation at this residue may disrupt this contact and thereby inhibit DNA binding by introduction of a negative charge. In addition, previous work has shown that two positively charged residues, Lys242 and Lys245 of FOXO1 (corresponding to Lys242 and Lys245 in FOXO3a) located in the C-terminal region of the DNA-binding domain, are prone to acetylation by CBP, leading to reduced DNA binding and increased sensitivity to PKB-induced phosphorylation at Ser253 (34). As shown in Figure 3C, Lys245 interacted directly with the DNA phosphate group, but Lys242 was too far away from the DNA to participate directly in binding. This is consistent with the results from our mutagenesis study (see below) where a K245A mutation resulted in a greater apparent loss of DNA binding than a K242A mutation. The protein–DNA interactions of Lys245 could be explained if the acetylation of Lys residues led to the reduction of the DNA-binding affinity. Interestingly, no apparent intramolecular interaction was found between the C-terminal coil and FOXO3a-DBD, suggesting that the C-terminal region is highly mobile in the absence of DNA. Hence, in the presence of DNA the C-terminal coil may be stabilized by interactions with the major groove. The C-terminal region of FOXO3a thus plays several important roles in DNA binding, and charge variations induced by phosphorylation or acetylation may attenuate the DNA-binding affinity of FOXO proteins.

Interaction between wing 1 and DNA

The FOXO3a-DBD/DNA complex structure revealed that wing 1 of FOXO3a also contributes to DNA binding by interacting with the phosphate backbone in the 3′-flanking region of the consensus sequence (Figure 3D). The terminal amine of Lys230 formed an ion pair with the phosphate group of T7′. In addition, the amide group of Ser232 made a hydrogen bond with the phosphate group of G6′. Arg222 and Trp234, located at the stem of wing 1, also made contact with the phosphate groups of G6′ (Figure 3D). Analysis of the amino acid composition of wing 1 of FOX proteins showed that FOXO3a is two residues shorter in the wing 1 region (Figure 1B). The lack of these two residues may change the shape and size of the wing 1 loop, such that wing 1 of FOXO3a is not long enough to push Lys230 far enough into the minor groove for DNA recognition. Thus, although wing 1 of FOXO3a may help to stabilize DNA binding, it does not play a direct role in protein–DNA recognition.

Structural comparison with other FOX proteins

A superimposition of the FOXO3a-DBD/DNA complex with the previously reported FOXA3, FOXK1a and FOXP2 DNA complexes showed a high degree of structural similarity in the core region (H1 ~ H3 and S1 ~ S3) with RMSDs of 0.64, 0.66 and 0.56 Å for Cα positions, respectively (Figure 5). However, there are several major structural deviations located in the H2–H3 turn, wing 1 and C-terminal regions, as the amino acid compositions and lengths of these regions are not well conserved. In the FOXA3 and FOXP2 complexes, both H2–H3 turns formed short α-helices. In contrast, the corresponding regions in FOXO3a and FOXK1a are coil structures. In particular, the H2–H3 turn region of FOXO3a has an insertion of five additional residues (198-GDSNS-202) that are solvent-exposed. The function of these extra residues is unknown, because there was no protein–DNA interaction in this region within the FOXO3a-DBD/DNA complex structure.

The wing 1 region of these FOX proteins also varies in sequence and length, which may lead to various conformations of the wing 1 structure (Figure 5). In the FOXK1a/DNA complex, wing 1 utilizes Lys73 (corresponding to Lys230 in FOXO3a) to insert into the minor

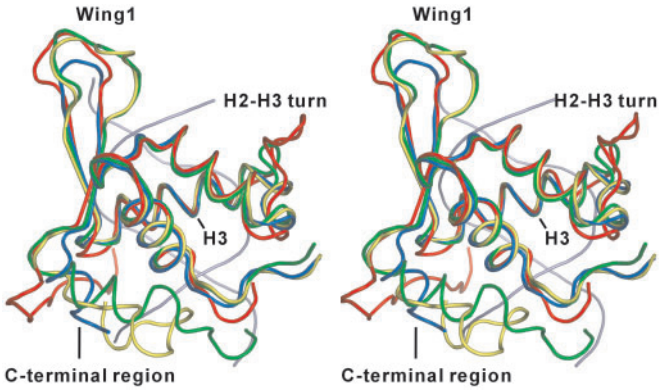

Figure 5. Structural comparison of FOXO3a-DBD with other FOX/DNA complexes. Stereo diagram of superposition of the FOXO3a, FOXA2, FOXK1a and FOXP2/DNA complexes showing the Cα trace. For clarity, only the DNA in FOXO3a-DBD is shown, in light blue. FOXO3a, FOXA3, FOXK1a and FOXP2 are shown in red, yellow, green and blue, respectively.

groove to recognize the base (35,36,41). In contrast to FOXK1a, no direct base interaction was found for residue Lys230 in the FOXO3a-DBD/DNA complex. However, in FOXP2, the five amino acids preceding the corresponding Lys residue were truncated, resulting in a simple turn that did not make any contact with DNA (41). Interestingly, in the FOXP3/NFAT/DNA ternary complex structure, the same Lys residue mediates a protein–protein interaction with NFAT (41). Due to the sequence variation in the wing 1 region, we speculate that the differences in length and amino acid composition of wing 1 allow it to play various roles in the mediation of DNA recognition, the stabilization of protein–DNA complex or the protein–protein interactions in the various FOX proteins.

The most structurally divergent region of these FOX/DNA complex structures is the C-terminus of the DNA-binding domains, which contains many positively charged residues and functions in DNA binding or recognition specificity. The C-terminal regions of FOXK1a and FOXP2 form an α-helix. In contrast, the corresponding regions of FOXO3a and FOXA3 adopt coiled structures. Although the C-terminal regions of FOXA3, FOXK1a and FOXP2 have different structures, they all position the protein in the same binding orientation, whereas the corresponding region in FOXO3a was in the opposite orientation (Figure 5). Due to the different arrangement of these coiled structures, FOXO3a interacted with DNA in the major groove whereas FOXA3 interacts with DNA in the minor groove.

DNA conformation in the FOXO3a-DBD/DNA complex

In the FOXO3a-DBD/DNA complex, the DNA exhibited a bend of 20° toward FOXO3a-DBD, mainly in the major groove, which was bound by the recognition helix. The base steps 2/3 and 6/7 were heavily kinked with roll angles 12.2° and 16.3°, respectively. The major groove was slightly wider (~3–4 Å wider than the canonical B-DNA) at positions where the recognition helix of FOXO3a-DBD was inserted. The minor groove was also slightly wider in the core sequence region. The helical twist per base pair varied from 24.0° to 40.5°. The DNA was 3.1% shorter than canonical B-DNA with the same number of nucleotides.

Mutational analyses of FOXO3a-DBD

To further characterize the roles of the residues involved in protein–DNA interactions in the FOXO3a-DBD/DNA structure, we studied the effect of various mutations on the ability of FOXO3a-DBD to bind to a DNA duplex containing either the FOXO consensus binding sequence 5′-GTAAACA-3′ or insulin response sequence (IRS) 5′-CAAAATA-3′ (50,51). Gel shift studies (Figure 6A and B) revealed that the FOXO3a-DBD$_{158–240}$ lacking the C-terminal region almost lost the ability to bind DNA, indicating that the C-terminal region of FOXO3a-DBD contributes significantly to the formation of a stable protein–DNA complex. Substitutions of the three basic residues (Arg248 ~ 250) with alanine also substantially diminished DNA binding. Because Lys242 and Lys245 are located in the C-terminus of FOXO3a-DBD, and Lys245 interacted with the phosphate group, we mutated these Lys residues to alanine and examined their effect on DNA binding. The K245A mutation reduced the DNA-binding ability more than the K242A mutation, consistent with the observed direct interaction between Lys245 and the DNA in the crystal structure. Although Lys242 did not contact the DNA, the K242A mutant showed a slight decrease in DNA affinity. We hypothesize that the K242A mutant impaired DNA binding by destabilizing the C-terminal region. We also examined the effect on DNA binding with the double mutant, K242A/K245A. Interestingly, DNA binding in this double mutant was dramatically reduced (Figure 6A and B), suggesting that K242 and K245 might have a synergistic effect on DNA binding.

Recently, CDK2 was shown to interact with the DNA-binding domain of FOXO1 by phosphorylating the C-terminus at Ser246 (corresponding to Ala246 in FOXO3a), which resulted in translocation from the nucleus to the cytoplasm (19). In the FOXO3a-DBD/DNA complex, Ala246 was close to the DNA major groove (Figure 3C). We constructed an aspartic acid substitution mutant, A246D, to mimic the Ser246-phosphorylated state of FOXO1 and to investigate its effect on DNA-binding ability. Indeed, the A246D mutant exhibited substantially decreased DNA binding, indicating that introduction of a negative charge at A246 reduced the DNA-binding ability of FOXO3a by decreasing the stability of the interaction between the C-terminus and DNA. In addition, we also created two mutants, K230A (wing 1 region) and R211A (recognition helix H3), to examine the importance of these residues in DNA binding. Both the R211A and K230A mutants showed an apparent loss of DNA-binding ability, consistent with the crystallographic data showing that both wing 1 and the C-terminal region of FOXO3a-DBD participated in DNA binding. Moreover, the FOXO consensus sequence had higher affinity for DNA than the IRS sequence, consistent with a previous report (50).

To compare the DNA-binding affinity of the FOXO3a-DBD proteins, we performed fluorescence anisotropy

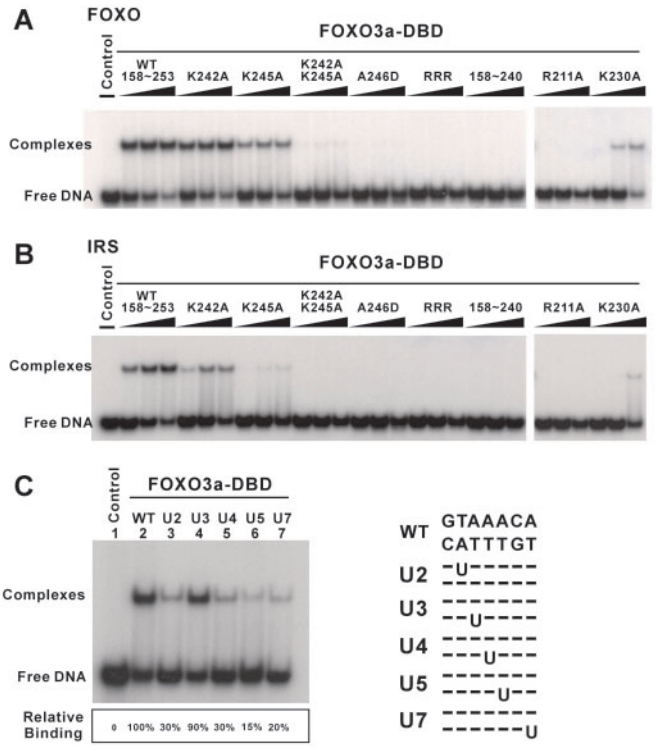

Figure 6. Electrophoretic mobility shift assay (EMSA). (**A**) EMSA was performed with wild-type, mutated and FOXO3a-DBD$_{158–240}$ and a ^{32}P-labeled oligonucleotide probe containing the FOXO consensus DNA-binding sequence, GTAAACA. In the control lane, only ^{32}P-labeled DNA was used. Free probe is indicated at the bottom of the gel. (**B**) DNA-binding affinity of wild-type, mutant and FOXO3a-DBD$_{158–240}$ with the insulin response sequence (IRS), CAAAACA. (**C**) EMSA of wild-type FOXO3a-DBD binding to oligonucleotides containing substitutions within the FOXO consensus sequence. Lane 1, ^{32}P-labeled DNA only; lanes 2–7, wild-type sequence or sequences substituted with U at positions 2, 3, 4, 5 or 7, respectively. The nucleotide sequence of each substitution site is shown on the right-hand side of Figure 6C. The final FOXO3a-DBD concentration in lanes 2–7 was 800 nM. The extent of FOXO3a-DBD relative binding to DNA (indicated below each lane) was quantified using a PhosphorImager (Molecular Dynamics). Lane 1 is a control, with no added protein. Positions of free DNA and the protein–DNA complex are indicated on the left.

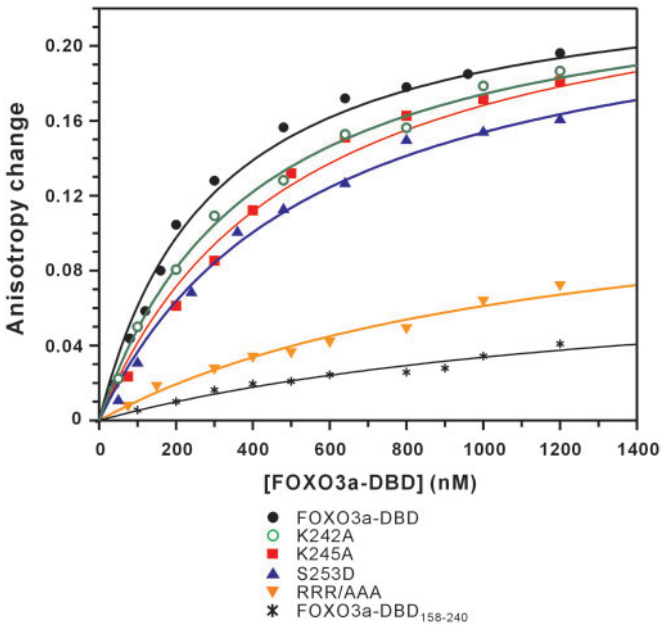

Figure 7. DNA-binding properties of FOXO3a-DBD proteins examined by fluorescence anisotropy assay. Wild-type FOXO3a-DBD$_{158–253}$, K242A, K245A, S253D, RRR/AAA and FOXO3a-DBD$_{158–240}$ were diluted and incubated with a fluorescein-labeled DNA at 25°C in 20 mM Tris–HCl, pH 7.6, NaCl 50 mM, DTT 1 mM. The anisotropy values were measured after 30 min incubation.

Table 2. DNA-binding properties of FOXO3a-DBD proteins[a]

Protein	K_d (nM)
WT (158–253)	295 ± 26
K242A	399 ± 25
K245A	511 ± 63
S253D	549 ± 55
RRR/AAA	1178 ± 168
WT (158–240)	1492 ± 197

[a]Measurements were performed in a 20 mM Tris–HCl, pH 7.6, 50 mM NaCl, 1 mM DTT at 25°C.

assay to measure the binding ability of these mutant proteins using a fluorescently labeled DNA containing the FOXO consensus binding sequence. As shown in Figure 7, we observed that the K24A and K245A mutants are defective in binding DNA compared to wild-type FOXO3a-DBD. The wild-type FOXO3a-DBD bound to DNA with an apparent K_d of 295 ± 26 nM (Table 2). However, the apparent K_d value for K242A and K245A mutants is 399 ± 25 nM and 511 ± 63 nM, respectively. These data support the results of gel shift studies that substitutions of K242 and K245 for alanine reduced the DNA-binding affinity of FOXO3a-DBD. In the structure, residue Ser253 interacted with phosphate group of DNA. To further study the role of PKB-induced phosphorylation at Ser253, we created a S253D mutant to mimic the phosphorylated state. The result showed that S253D mutant caused a decrease on its DNA-binding ability (K_d = 511 ± 63 nM), indicating that phosphorylation at Ser253 influences the stability of protein–DNA interaction. This effect is also consistent with the result that S256D of FOXO1 (Ser253 in FOXO3a) led a decrease in DNA-binding affinity (52). In addition, substitutions of the three basic residues (Arg248 ~ 250) with alanine also significantly impaired DNA-binding affinity with an apparent K_d of 1178 ± 168 nM. Furthermore, the truncation of C-terminus at the FOXO3a-DBD also caused a 5-fold decrease for DNA-binding (K_d = 1492 ± 197 nM), indicating that the C-terminus of FOXO3a-DBD is important for DNA binding.

FOXO protein recognizes an AT-rich consensus sequence

In the FOXO3a-DBD/DNA structure, methyl groups of thymine bases within the 5′-GTAAACA-3′ consensus sequence formed numerous van der Waals contacts with the recognition helix. This phenomenon suggested that

these methyl groups are also important for FOXO protein recognition of the AT-rich consensus DNA. To test this hypothesis and analyze the binding contribution from each methyl group, we substituted individual T nucleotides with U and measured the affinity of wild-type FOXO3a-DBD for the new oligonucleotides. As shown in Figure 6C, the substitution U2 decreased protein–DNA complex formation to 30%, whereas base substitution at positions U4, U5 and U7 reduced binding to 30, 15 and 20%, respectively. Base substitution at position U3 did not apparently decrease in DNA binding, which was consistent with the structure result where no interaction was found between the methyl group of T3′ and the recognition helix (Figure 3A). In the FOXO3a-DBD/DNA complex structure, the methyl groups of DNA bases T5′ and T7′ interacted with residue Arg211 through van der Waals contacts (Figures 3A and 4), which explained why the R211A mutant in FOXO3a-DBD had substantially less affinity for DNA. Based on the structure and on these DNA substitution experiments, we suggest that van der Waals contacts between the methyl groups of thymine bases and side chains of the recognition helix are important for FOXO3a recognition of the FOXO consensus sequence.

DISCUSSION

Previously reported structures of FOX proteins bound to DNA revealed the presence of basic amino acids at the C-terminal region of forkhead DNA-binding domains that play an important role in DNA binding (35,36,41). In the FOXO family, the C-terminal basic region of the DNA-binding domain contains several post-modification sites and is a direct target of the PI3K–PKB signaling pathway in response to insulin or growth factors (20,22,23). PKB-induced phosphorylation and CBP-induced acetylation at the C-terminus of FOXO-DBD have been shown to alter its transcriptional activity (21,34). These C-terminal post-transcriptional modifications allow for regulation of FOXO-DBD transcriptional activity by altering its DNA-binding affinity. Hence, the goal of this work was to find the molecular basis by which FOXO-DBD interacts with DNA and help explain why the DNA-binding properties of FOXO proteins can be altered by phosphorylation and acetylation within the NLS.

Regulation of FOXO by the PI3K–PKB pathway

The FOXO family is a key downstream target of the PI3K–PKB pathway in response to cellular stimulation by insulin or growth factors (20). PKB-induced phosphorylation at three regulatory sites (Thr32, Ser253 and Ser315 in FOXO3a) results in the export of FOXO proteins from the nucleus to the cytoplasm (20). Among these three phosphorylation sites, Ser253 is the primary site located within the NLS of FOXO proteins which overlaps with the 14-3-3 binding motif. PKB-induced phosphorylation at Ser253 and the sequential binding of 14-3-3 proteins have been suggested to prevent the interaction of FOXO with its target genes (20). In support of this hypothesis, our study showed that replacing a cluster of three basic residues adjacent to Ser253 in the C-terminal region (corresponding to Arg248, Arg249 and Arg250 in FOXO3a) with neutral amino acids effectively disrupted DNA binding by FOXO3a-DBD (Figures 6A, B and 7). These findings are consistent with our FOXO3a-DBD/DNA complex structure showing that all three basic residues (Arg248, Arg249 and Arg250) and Ser253 interact with the phosphate groups of the DNA major groove (Figure 3B). These interactions may also explain how the binding of 14-3-3 following phosphorylation of Ser253 can mask the interaction of the above four residues to prevent their interaction with DNA, resulting in a decrease in DNA-binding affinity.

Recently, FOXO protein acetylation was shown to attenuate their transcriptional activity (21,31,32). In particular, the three FOXO C-terminal Lys residues Lys242, Lys245 and Lys262, which correspond to Lys242, Lys245 and Lys259 of FOXO3a, can be acetylated by CBP to decrease the DNA affinity and increase the sensitivity for phosphorylation of Ser253 by PKB (34). The structure of the FOXO3a-DBD/DNA complex revealed that Lys245 directly interacted with the phosphate group of DNA, but the side chain of Lys242 was exposed to the solvent rather than binding to DNA (Figure 3C). This result was also in agreement with our mutagenesis study, which showed that the DNA-binding affinity of K245A was much less than that of K242A (Figures 6A, B and 7). Therefore, acetylation of K245, located in the C-terminus of FOXO-DBD, may disrupt the protein–DNA contacts, resulting in destabilization of this region and providing increased opportunity for PKB to phosphorylate Ser253. In the FOXO3a-DBD/DNA structure, the C-terminus of the DBD formed a random coil that interacted with the negatively charged phosphate groups in the DNA major groove. Interestingly, this proposed coiled structure for the C-terminus of FOXO-DBD is consistent with previous studies where the peptides used to recognize 14-3-3 also adopted coil structures (53). From these results, we suggest that the C-terminal region of the DNA-binding domain of FOXO proteins is crucial for effective DNA binding and that the sequential events of PKB-induced phosphorylation, the binding of 14-3-3 protein, and CBP-induced acetylation in this region can inhibit binding of the C-terminus to DNA.

DNA sequence preference in the FOXO family

Our study revealed that FOXO3a-DBD bound to a FOXO consensus DNA-binding site. The consensus binding sequence for FOXO proteins is 5′-GTAAA(C/T)A-3′ (50). Previous studies have shown that the characterized FOXO binding sites within promoters of growth factor-responsive genes contain either the FOXO consensus binding sequence or the IRS (5′-CAAAA(C/T)A-3′) (50,51). Comparison of the FOXO and IRS sequences showed that both of these sequences encompass a 5′-AAA(C/T)A-3′ binding motif and contain several adenine residues, suggesting that the 5′-AAA(C/T)A-3′ sequence is important for DNA

recognition by FOXO proteins. Here, we used this consensus binding sequence in structural and biochemical studies to explain why the preferred DNA-binding sequences of FOXO proteins are AT-rich.

At the interface between the recognition helix H3 and the major groove, the A–T base pair at position 3 (GTAAACA) was recognized by His212 via a hydrogen bond to the T3′ base. Meanwhile, substitution of T3′ by U caused only a slight decrease in DNA-binding affinity, indicating that the specificity of T3′ was mainly contributed by His212 via hydrogen bonding rather than van der Waals forces. In the site selection studies, the A–T base pair at position 4 (GTAAACA) was highly preferred in some binding sites of the previously characterized FOX proteins (42,50,54). In the FOXO3a-DBD/DNA complex, the A4 base was contacted by the highly conserved residue, Asn208, through two direct hydrogen bonds. In addition, its base-pair partner T4′ interacted with Ser215, which provided a van der Waals contact with the T4′ methyl group and resulted in effective discrimination of A from G at this position. Our study also showed that substitution of T4′ with U decreased DNA affinity. For the A–T base pairs at positions 5 and 7 (GTAAACA), Arg211 contacted the T5′ and T7′ methyl groups only through van der Waals forces. We also substituted U at positions T5′ or T7′ and constructed an R211A mutant and analyzed the effects on DNA affinity. These substitutions and the R211A mutant severely impaired the DNA-binding ability of FOXO3a-DBD (Figure 6A and B), suggesting that the methyl groups of base T5′ and T7′ are crucial for recognition by Arg211.

Our results show that the DNA recognition specificity of FOXO3a is due to a series of van der Waals contacts between the methyl groups of thymine bases and the side chains of Arg211, Ser215 and His212 within the recognition helix. As shown in Figure 1B, these residues are absolutely conserved in FOXO proteins, suggesting that similar contacts may be observed in other members of FOXO family. Hence, we speculate that the methyl groups of thymine in the FOXO consensus DNA-binding sequence play an important role in promoter recognition by FOXO proteins.

In summary, our structure of the FOXO3a-DBD/DNA complex provides a good molecular model for FOXO-DBD binding to the consensus DNA-binding sequence. In addition to the recognition helix H3, structural and biochemical analyses also reveal that both wing 1 and the C-terminal regions contribute to DNA binding. The C-terminus of FOXO3a-DBD, which functions as a NLS and contains a PKB phosphorylation site and 14-3-3 binding motif, adopts a coil structure inserted into the major groove of DNA. These results reveal that the C-terminal region of FOXO3a-DBD plays a crucial role in stabilizing the formation of the complex with DNA. The structure of this complex provides insight into how PKB-induced phosphorylation, 14-3-3 protein binding and CBP-induced acetylation can alter the transcriptional activity of FOXO proteins by attenuating DNA affinity.

PDB accession code

The atomic coordinates of FOXO3a-DBD/DNA complex have been deposited in the Protein Data Bank under accession code 2uzk.

ACKNOWLEDGEMENTS

We gratefully acknowledge access to the synchrotron radiation beamline 13B1 at the National Synchrotron Radiation Research Center (NSRRC) in Taiwan. This work was supported by research grants from Academia Sinica and the National Science Council (NSC95-2311-B-001-064 to C.-D.H.), Taiwan, Republic of China. Funding to pay the Open Access publication charges for this article was provided by National Science Council, Taiwan, Republic of China.

Conflict of interest statement. None declared.

REFERENCES

1. Kaufmann,E. and Knochel,W. (1996) Five years on the wings of fork head. *Mech. Dev.*, **57**, 3–20.
2. Hromas,R. and Costa,R. (1995) The hepatocyte nuclear factor-3/forkhead transcription regulatory family in development, inflammation, and neoplasia. *Crit. Rev. Oncol. Hematol.*, **20**, 129–140.
3. Lai,E., Clark,K.L., Burley,S.K. and Darnell,J.E.Jr (1993) Hepatocyte nuclear factor 3/fork head or ''winged helix'' proteins: a family of transcription factors of diverse biologic function. *Proc. Natl Acad. Sci. USA*, **90**, 10421–10423.
4. Granadino,B., Perez-Sanchez,C. and Rey-Campos,J. (2000) Fork head transcription factors. *Curr. Genomics*, **1**, 353–382.
5. Barthel,A., Schmoll,D. and Unterman,T.G. (2005) FoxO proteins in insulin action and metabolism. *Trends Endocrinol. Metab.*, **16**, 183–189.
6. Accili,D. and Arden,K.C. (2004) FoxOs at the crossroads of cellular metabolism, differentiation, and transformation. *Cell*, **117**, 421–426.
7. Van Der Heide,L.P., Hoekman,M.F. and Smidt,M.P. (2004) The ins and outs of FoxO shuttling: mechanisms of FoxO translocation and transcriptional regulation. *Biochem. J.*, **380**, 297–309.
8. Arden,K.C. (2004) FoxO: linking new signaling pathways. *Mol. Cell*, **14**, 416–418.
9. Kops,G.J., Dansen,T.B., Polderman,P.E., Saarloos,I., Wirtz,K.W., Coffer,P.J., Huang,T.T., Bos,J.L., Medema,R.H. *et al.* (2002) Forkhead transcription factor FOXO3a protects quiescent cells from oxidative stress. *Nature*, **419**, 316–321.
10. Burgering,B.M. and Kops,G.J. (2002) Cell cycle and death control: long live forkheads. *Trends Biochem. Sci.*, **27**, 352–360.
11. Jacobs,F.M., van der Heide,L.P., Wijchers,P.J., Burbach,J.P., Hoekman,M.F. and Smidt,M.P. (2003) FoxO6, a novel member of the FoxO class of transcription factors with distinct shuttling dynamics. *J. Biol. Chem.*, **278**, 35959–35967.
12. Anderson,M.J., Viars,C.S., Czekay,S., Cavenee,W.K. and Arden,K.C. (1998) Cloning and characterization of three human forkhead genes that comprise an FKHR-like gene subfamily. *Genomics*, **47**, 187–199.
13. Galili,N., Davis,R.J., Fredericks,W.J., Mukhopadhyay,S., Rauscher,F.J.III, Emanuel,B.S., Rovera,G. and Barr,F.G. (1993) Fusion of a fork head domain gene to PAX3 in the solid tumour alveolar rhabdomyosarcoma. *Nat. Genet.*, **5**, 230–235.
14. Borkhardt,A., Repp,R., Haas,O.A., Leis,T., Harbott,J., Kreuder,J., Hammermann,J., Henn,T. and Lampert,F. (1997) Cloning and characterization of AFX, the gene that fuses to MLL in acute leukemias with a t(X;11)(q13;q23). *Oncogene*, **14**, 195–202.
15. Greer,E.L. and Brunet,A. (2005) FOXO transcription factors at the interface between longevity and tumor suppression. *Oncogene*, **24**, 7410–7425.

16. Hu,M.C., Lee,D.F., Xia,W., Golfman,L.S., Ou-Yang,F., Yang,J.Y., Zou,Y., Bao,S., Hanada,N. *et al.* (2004) IkappaB kinase promotes tumorigenesis through inhibition of forkhead FOXO3a. *Cell*, **117**, 225–237.
17. Potente,M., Urbich,C., Sasaki,K., Hofmann,W.K., Heeschen,C., Aicher,A., Kollipara,R., DePinho,R.A., Zeiher,A.M. *et al.* (2005) Involvement of Foxo transcription factors in angiogenesis and postnatal neovascularization. *J. Clin. Invest.*, **115**, 2382–2392.
18. Aoki,M., Jiang,H. and Vogt,P.K. (2004) Proteasomal degradation of the FoxO1 transcriptional regulator in cells transformed by the P3k and Akt oncoproteins. *Proc. Natl Acad. Sci. USA*, **101**, 13613–13617.
19. Huang,H., Regan,K.M., Lou,Z., Chen,J. and Tindall,D.J. (2006) CDK2-dependent phosphorylation of FOXO1 as an apoptotic response to DNA damage. *Science*, **314**, 294–297.
20. Brunet,A., Bonni,A., Zigmond,M.J., Lin,M.Z., Juo,P., Hu,L.S., Anderson,M.J., Arden,K.C., Blenis,J. *et al.* (1999) Akt promotes cell survival by phosphorylating and inhibiting a forkhead transcription factor. *Cell*, **96**, 857–868.
21. Daitoku,H., Hatta,M., Matsuzaki,H., Aratani,S., Ohshima,T., Miyagishi,M., Nakajima,T. and Fukamizu,A. (2004) Silent information regulator 2 potentiates Foxo1-mediated transcription through its deacetylase activity. *Proc. Natl Acad. Sci. USA*, **101**, 10042–10047.
22. Takaishi,H., Konishi,H., Matsuzaki,H., Ono,Y., Shirai,Y., Saito,N., Kitamura,T., Ogawa,W., Kasuga,M. *et al.* (1999) Regulation of nuclear translocation of forkhead transcription factor AFX by protein kinase B. *Proc. Natl Acad. Sci. USA*, **96**, 11836–11841.
23. Kops,G.J., de Ruiter,N.D., De Vries-Smits,A.M., Powell,D.R., Bos,J.L. and Burgering,B.M. (1999) Direct control of the forkhead transcription factor AFX by protein kinase B. *Nature*, **398**, 630–634.
24. Brunet,A., Kanai,F., Stehn,J., Xu,J., Sarbassova,D., Frangioni,J.V., Dalal,S.N., DeCaprio,J.A., Greenberg,M.E. *et al.* (2002) 14-3-3 transits to the nucleus and participates in dynamic nucleocytoplasmic transport. *J. Cell Biol.*, **156**, 817–828.
25. Cahill,C.M., Tzivion,G., Nasrin,N., Ogg,S., Dore,J., Ruvkun,G. and Alexander-Bridges,M. (2001) Phosphatidylinositol 3-kinase signaling inhibits DAF-16 DNA binding and function via 14-3-3-dependent and 14-3-3-independent pathways. *J. Biol. Chem.*, **276**, 13402–13410.
26. Obsil,T., Ghirlando,R., Anderson,D.E., Hickman,A.B. and Dyda,F. (2003) Two 14-3-3 binding motifs are required for stable association of forkhead transcription factor FOXO4 with 14-3-3 proteins and inhibition of DNA binding. *Biochemistry*, **42**, 15264–15272.
27. Zhao,X., Gan,L., Pan,H., Kan,D., Majeski,M., Adam,S.A. and Unterman,T.G. (2004) Multiple elements regulate nuclear/cytoplasmic shuttling of FOXO1: characterization of phosphorylation- and 14-3-3-dependent and -independent mechanisms. *Biochem. J.*, **378**, 839–849.
28. Brownawell,A.M., Kops,G.J., Macara,I.G. and Burgering,B.M. (2001) Inhibition of nuclear import by protein kinase B (Akt) regulates the subcellular distribution and activity of the forkhead transcription factor AFX. *Mol. Cell. Biol.*, **21**, 3534–3546.
29. Obsilova,V., Vecer,J., Herman,P., Pabianova,A., Sulc,M., Teisinger,J., Boura,E. and Obsil,T. (2005) 14-3-3 Protein interacts with nuclear localization sequence of forkhead transcription factor FoxO4. *Biochemistry*, **44**, 11608–11617.
30. Motta,M.C., Divecha,N., Lemieux,M., Kamel,C., Chen,D., Gu,W., Bultsma,Y., McBurney,M. and Guarente,L. (2004) Mammalian SIRT1 represses forkhead transcription factors. *Cell*, **116**, 551–563.
31. van der Horst,A., Tertoolen,L.G., de Vries-Smits,L.M., Frye,R.A., Medema,R.H. and Burgering,B.M. (2004) FOXO4 is acetylated upon peroxide stress and deacetylated by the longevity protein hSir2(SIRT1). *J. Biol. Chem.*, **279**, 28873–28879.
32. Fukuoka,M., Daitoku,H., Hatta,M., Matsuzaki,H., Umemura,S. and Fukamizu,A. (2003) Negative regulation of forkhead transcription factor AFX (Foxo4) by CBP-induced acetylation. *Int. J. Mol. Med.*, **12**, 503–508.
33. Brunet,A., Sweeney,L.B., Sturgill,J.F., Chua,K.F., Greer,P.L., Lin,Y., Tran,H., Ross,S.E., Mostoslavsky,R. *et al.* (2004) Stress-dependent regulation of FOXO transcription factors by the SIRT1 deacetylase. *Science*, **303**, 2011–2015.
34. Matsuzaki,H., Daitoku,H., Hatta,M., Aoyama,H., Yoshimochi,K. and Fukamizu,A. (2005) Acetylation of Foxo1 alters its DNA-binding ability and sensitivity to phosphorylation. *Proc. Natl Acad. Sci. USA*, **102**, 11278–11283.
35. Clark,K.L., Halay,E.D., Lai,E. and Burley,S.K. (1993) Co-crystal structure of the HNF-3/fork head DNA-recognition motif resembles histone H5. *Nature*, **364**, 412–420.
36. Tsai,K.L., Huang,C.Y., Chang,C.H., Sun,Y.J., Chuang,W.J. and Hsiao,C.D. (2006) Crystal structure of the human FOXK1a–DNA complex and its implications on the diverse binding specificity of winged helix/forkhead proteins. *J. Biol. Chem.*, **281**, 17400–17409.
37. Jin,C. and Liao,X. (1999) Backbone dynamics of a winged helix protein and its DNA complex at different temperatures: changes of internal motions in genesis upon binding to DNA. *J. Mol. Biol.*, **292**, 641–651.
38. Gajiwala,K.S. and Burley,S.K. (2000) Winged helix proteins. *Curr. Opin. Struct. Biol.*, **10**, 110–116.
39. Weigelt,J., Climent,I., Dahlman-Wright,K. and Wikstrom,M. (2001) Solution structure of the DNA binding domain of the human forkhead transcription factor AFX (FOXO4). *Biochemistry*, **40**, 5861–5869.
40. Jin,C., Marsden,I., Chen,X. and Liao,X. (1999) Dynamic DNA contacts observed in the NMR structure of winged helix protein–DNA complex. *J. Mol. Biol.*, **289**, 683–690.
41. Stroud,J.C., Wu,Y., Bates,D.L., Han,A., Nowick,K., Paabo,S., Tong,H. and Chen,L. (2006) Structure of the forkhead domain of FOXP2 bound to DNA. *Structure*, **14**, 159–166.
42. Pierrou,S., Hellqvist,M., Samuelsson,L., Enerback,S. and Carlsson,P. (1994) Cloning and characterization of seven human forkhead proteins: binding site specificity and DNA bending. *EMBO J.*, **13**, 5002–5012.
43. Overdier,D.G., Porcella,A. and Costa,R.H. (1994) The DNA-binding specificity of the hepatocyte nuclear factor 3/forkhead domain is influenced by amino-acid residues adjacent to the recognition helix. *Mol. Cell. Biol.*, **14**, 2755–2766.
44. Otwinowski,Z. and Minor,W. (1997) Processing of X-ray diffraction data collected in oscillation Mode. *Methods Enzymol.*, **276**, 307–326.
45. Vagin,A. and Teplyakov,A. (1997) MOLREP: an automated program for molecular replacement. *J. Appl. Cryst.*, **30**, 1022–1025.
46. McRee,D.E. (1999) XtalView/Xfit—A versatile program for manipulating atomic coordinates and electron density. *J. Struct. Biol.*, **125**, 156–165.
47. Brunger,A.T., Adams,P.D., Clore,G.M., DeLano,W.L., Gros,P., Grosse-Kunstleve,R.W., Jiang,J.S., Kuszewski,J., Nilges,M. *et al.* (1998) Crystallography & NMR system: a new software suite for macromolecular structure determination. *Acta Crystallogr. D. Biol. Crystallogr.*, **54**, 905–921.
48. Lavery,R. and Sklenar,H. (1989) Defining the structure of irregular nucleic acids: conventions and principles. *J. Biomol. Struct. Dyn.*, **6**, 655–667.
49. DeLano,W.L. (2002) *The PyMOL User's Manual.* Delano Scientific, San Carlos, CA.
50. Furuyama,T., Nakazawa,T., Nakano,I. and Mori,N. (2000) Identification of the differential distribution patterns of mRNAs and consensus binding sequences for mouse DAF-16 homologues. *Biochem. J.*, **349**, 629–634.
51. Cichy,S.B., Uddin,S., Danilkovich,A., Guo,S., Klippel,A. and Unterman,T.G. (1998) Protein kinase B/Akt mediates effects of insulin on hepatic insulin-like growth factor-binding protein-1 gene expression through a conserved insulin response sequence. *J. Biol. Chem.*, **273**, 6482–6487.
52. Zhang,X., Gan,L., Pan,H., Guo,S., He,X., Olson,S.T., Mesecar,A., Adam,S. and Unterman,T.G. (2002) Phosphorylation of serine 256 suppresses transactivation by FKHR (FOXO1) by multiple mechanisms. Direct and indirect effects on nuclear/cytoplasmic shuttling and DNA binding. *J. Biol. Chem.*, **277**, 45276–45284.
53. Yaffe,M.B., Rittinger,K., Volinia,S., Caron,P.R., Aitken,A., Leffers,H., Gamblin,S.J., Smerdon,S.J. and Cantley,L.C. (1997) The structural basis for 14-3-3: phosphopeptide binding specificity. *Cell*, **91**, 961–971.
54. Kaufmann,E., Muller,D. and Knochel,W. (1995) DNA recognition site analysis of xenopus winged helix proteins. *J. Mol. Biol.*, **248**, 239–254.